Research article

Jiaoqi Huang, Yang Zhang, Zhongquan Lin, Wei Liu, Xueping Chen, Yu Liu, Huiyan Tian, Qiqian Liu, Raymond Gillibert, Jolanda Spadavecchia, Nadia Djaker, Marc Lamy de la Chapelle, Yang Xiang* and Weiling Fu*

Femtomolar detection of nucleic acid based on functionalized gold nanoparticles

https://doi.org/10.1515/nanoph-2019-0050
Received February 20, 2019; revised April 11, 2019; accepted April 13, 2019

Abstract: Deoxyribonucleic acid (DNA) detection is essential for the accurate and early diagnosis of a disease. In this study, a femtomolar DNA detection method based on the exploitation of the localized surface plasmon (LSP) resonance of gold nanoparticles (AuNPs) was developed. We prepared Poly Ethylen Glycol (PEG) functionalized AuNPs with a specific DNA capture probe (CP) directly modified on the gold surface. Two strategies are proposed using different kinds of CP to detect the target DNA (tDNA). In the first strategy, CP is the complementary of the complete sequence of the DNA (CCP method). For the second strategy, we used two CPs, which were half complementary to tDNA, and these were hybridized with tDNA to form sandwich structures (MIX method). The results showed that our detection methods are highly sensitive and that the limits of detection of 124 aM and 2.54 fM tDNA can be reached when using the CCP and MIX methods, respectively. In addition, the specificity of our two strategies is also demonstrated with mismatched DNAs. The proposed method provides a simple, fast, sensitive and specific DNA biosensor, which has the potential to be used for point-of-care tests (POCT).

Keywords: DNA detection; surface plasmon; gold nanoparticle.

***Corresponding authors: Yang Xiang,** Department of Laboratory Medicine, Southwest Hospital, Third Military Medical University (Army Medical University), No. 29 Gaotanyan street, Shapingba, Chongqing 400038, China; and Department of Clinical Microbiology and Immunology, Faculty of Pharmacy and Medical Laboratory Sciences, Third Military Medical University (Army Medical University), Chongqing 400038, China, e-mail: xyang_@hotmail.com; and **Weiling Fu,** Department of Laboratory Medicine, Southwest Hospital, Third Military Medical University (Army Medical University), No. 29 Gaotanyan street, Shapingba, Chongqing 400038, China, e-mail: fwl@tmmu.edu.cn
Jiaoqi Huang, Zhongquan Lin, Wei Liu, Xueping Chen, Yu Liu and Huiyan Tian: Department of Laboratory Medicine, Southwest Hospital, Third Military Medical University (Army Medical University), Chongqing 400038, China
Yang Zhang: Department of Laboratory Medicine, Chongqing General Hospital, Chongqing 400038, China
Qiqian Liu, Raymond Gillibert, Jolanda Spadavecchia and Nadia Djaker: Université Paris 13, Sorbonne Paris Cité, UFR SMBH, Laboratoire CSPBAT, CNRS (UMR 7244), 74 rue Marcel Cachin, F-93017 Bobigny, France
Marc Lamy de la Chapelle: Department of Laboratory Medicine, Southwest Hospital, Third Military Medical University (Army Medical University), Chongqing 400038, China; and Institut des Molécules et Matériaux du Mans (IMMM – UMR CNRS 6283), Université du Mans, Avenue Olivier Messiaen, 72085 Le Mans, France

1 Introduction

Deoxyribonucleic acid (DNA) is one of the most important biomolecules in various life forms. It stores and transmits genetic information to control biological development and vital functions. As DNA plays and important role in regulating vital biological processes, they can be used as important biomarkers for biological studies and medical diagnostics [1–4]. Over the past three decades, several detection methods for specific DNA sequences have been developed. Polymerase chain reaction (PCR) is the most well-known nucleic acid amplification technology; it is widely used in practical applications and is especially suitable for trace nucleic acid detection [5]. However, PCR needs a precise temperature cycling protocol and a sophisticated design of primer, which makes it difficult to be used in point-of-care test (POCT). The isothermal amplification of nucleic acids has emerged as a promising alternative of PCR [6], including rolling circle amplification (RCA) [7], loop-mediated amplification (LAMP) [8], helicase-dependent amplification reaction (HDA) [9] and exponential amplification reaction (EXPAR) [10]. As only a single temperature is required, which can be achieved

by a simple water bath, the isothermal nucleic acid amplification has great potential for achieving low-cost, rapid point-of-care molecular diagnosis.

At the same time, benefiting from rapid advances in biotechnology, chemistry and nanotechnology, many novel readout strategies have been introduced into the field of biomarker detection, such as electrochemistry [11, 12], spectroscopy [13], colorimetric [14, 15], surface plasmon resonance (SPR) [16] and surface enhancement raman spectroscopy (SERS) [17–22]. In early studies, researchers have attempted to use a simple system for DNA detection. Tan et al. [23] combined isothermal DNA amplification with AuNPs for colorimetric detection. They observed a direct color change from red to blue and a detection of 100 fM oligonucleotide. He et al. [24] took advantage of the big surface and high dielectric constant of gold nanoparticles (AuNPs) to improve the sensitivity of SPR DNA sensor, and they achieved a ~10 pM limit of quantitation. Su et al. [25] developed a gold-silver bimetallic nanomushroom to act as a DNA probe, which promoted the SERS signal and was expected to realize multiplex detection. However, they reported that the complex nanostructure was not easy to synthesize and control. The exploitation of localized surface plasmon (LSP) resonance of AuNPs as transducers has competitive advantages, such as high sensitivity, simplicity, fast detection and miniaturized platform, which are all suitable for POCT [26–29].

LSP is the resonant oscillation of free electrons inside noble metal NPs stimulated by incident light. The excitation of the LSP is a light-matter interaction and exhibits a resonance behavior at a specific wavelength known as the LSP resonance (LSPR) [30, 31]. As the LSP can be seen as a resonator, the position of the LSPR is highly sensitive to any modification of the local environment that induces a shift of the LSPR. Thus, the observation of any LSPR shift can be employed to detect disease-related biomarkers, such as proteins and oligonucleotides, etc. [32]. According to such a readout, there are two LSPR sensing strategies. The first one is based on the sensitivity of the LSPR to changes in the dielectric constant of the surrounding medium or adsorbents. Any addition or interaction of some analytes at the nanoparticle surface results in the modification of the local dielectric constant or refractive index around the NPs, which will induce a redshift of the LSPR. The second sensing strategy is based on inter-particle coupling effect. The aggregation of the NPs results in the observation of a specific band at higher wavelength than for the individual NPs. The aggregation or dissociation of the NPs induces an intensity change of this "coupling" LSPR that can be related to the concentrations of the added analytes. However, these label-free LSPR assays show moderate sensitivity, generally at the nanomolar level for DNA detection [33]. For most clinical samples, highly sensitive DNA assays are needed for early detection and accurate diagnosis of disease.

In this study, we employed AuNPs covered by Poly Ethylen Glycol (PEG) as an effective LSPR platform to detect single-strand DNAs (ssDNA). In the following, our targeted DNA will be called tDNA. The PEG is used to maintain the stability of the AuNPs in complex samples and to prevent the complete aggregation after the addition of tDNA [34]. Another important function of PEG is to improve the efficiency of the capture probe (CP) in capturing tDNA on the surface of the AuNPs [35]. For the tDNA detection, we proposed two different strategies (Figure 1). For the first strategy (CCP method, 3b), we used one oligonucleotide CP, whose sequence is the complementary of the complete sequence of the tDNA (this is called complete capture probe or ccpDNA). For the second strategy (MIX method, 3c), we used two oligonucleotides, whose sequences are the complementary of the half of the tDNA sequence as the CP: one CP corresponds to the first half part of the tDNA (called hcpDNA1), whereas the other corresponds to the second half of the tDNA (called hcpDNA2). We determined and compared the sensing performances of both strategies in terms of sensitivity, limit of detection (LoD) and operating range. We demonstrated that both strategies show the potential to minimize the nonspecific detection and to improve the sensitivity simultaneously.

2 Experimental

2.1 Material

The tetrachloroauric acid ($HAuCl_4$), sodium borohydride ($NaBH_4$), dicarboxylic Poly Ethylene Glycol-200 (PEG) and phosphate-buffered solution (PBS), were all provided by Sigma Aldrich (St. Louis, MO, USA) at maximum purity grade. All oligonucleotides used in this study (Table 1) were synthesized and purified by high performance liquid chromatography (HPLC) from Sangon Biotech (Shanghai, China). All chemicals employed were of analytical reagent grade. High-purity deionized water prepared by a Milli-Q water purification system (Millipore Corp., Bedford, USA) was used for all experiments.

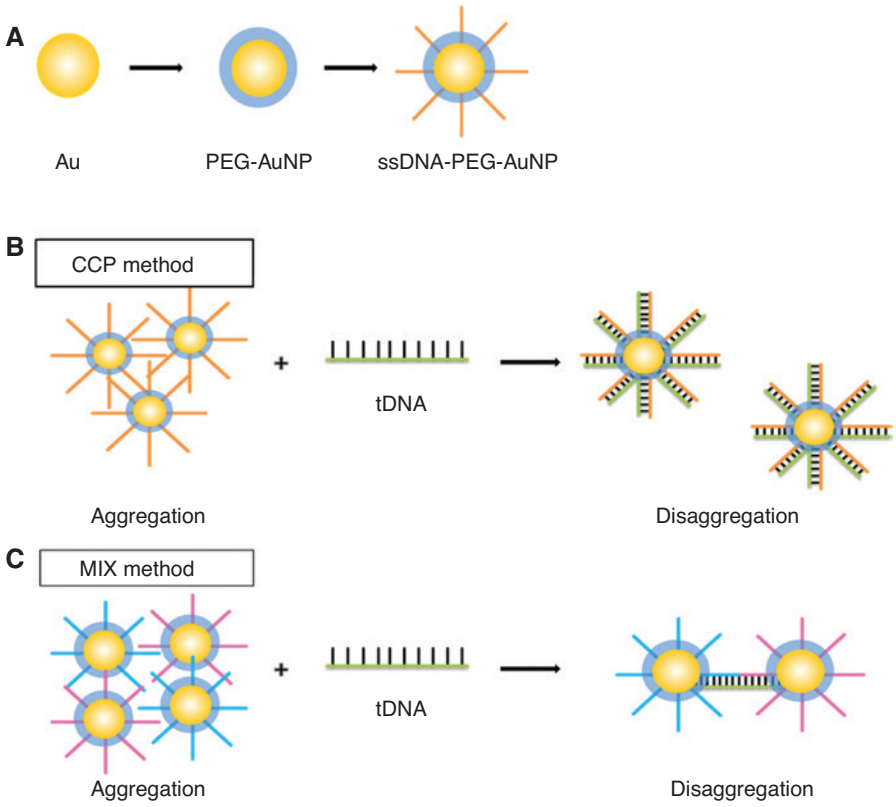

Figure 1: The schemes for the tDNA detection.
(A) The colloidal gold nanoparticles (AuNPs) are encoded with low molecular weight polyethylene glycols (PEG) and functionalized with thiolated DNA capture probes (ccpDNA, hcpDNA-1 or hcpDNA-2). (B) The CCP detection method with the complete capture probe (ccpDNA) grafted at the gold nanoparticle surface: the disaggregation of the NPs is induced by the direct binding between the ccpDNA and the target DNA (tDNA). (C) The MIX method using both the half-capture probes (hcpDNA-1 and hcpDNA-2) grafted separately on different NPs: the disaggregation of the NPs is induced by one tDNA molecule binding to two NPs. Each gold particle contains about half complementation bases of the tDNA.

Table 1: The oligonucleotide sequences used in this study.

Oligonucleotide	Sequence (5′-3′)
tDNA	TAGCTTATCAGACTGATGTTGA
ccpDNA	TCAACATCAGTCTGATAAGCTATTTTTTTTT-SH
hcpDNA1	CTGATAAGCTA-TTTTTTTT-S H
hcpDNA2	SH-TTTTTTTT-TCAACATCAGT
M4T	TAGCCTGTCAGACTGTTCTTGA
NC	GCAACATCGATCTCTTAAGCTA

2.2 DNA capture probes

We designed the DNA capture probes with specific sequences including two components: the first 9 nucleotides served as a flexible spacer and the following sequence served as a recognition element for the tDNA. In the recognition part, we designed three different sequences based on our two detection strategies. First, the ccp-DNA capture probe had an equal length than the tDNA and was completely complementarity (Table 1). The two hcpDNA capture probes contained half complementation bases of the tDNA (Table 1). All of these aligned in a tail-to-tail fashion onto the complementary target polynucleotide.

2.3 Synthesis of PEG-AuNPs

The colloidal solutions of AuNPs coated with PEG (PEG-AuNPs) were prepared by a well assessed chemical reduction process according to previously described procedure [34]. Briefly, 20 ml of chloroauric acid ($HAuCl_4$, 10^{-3} M) aqueous solution was added to 1 ml of dicarboxylic PEG and mixed by magnetic stirring for 10 min at room temperature. To this solution, 6 ml of aqueous 0.01 M $NaBH_4$ was added at once. The color turned from yellow into ruby red. The resulting solution was stored away from light in the −4°C for later use.

2.4 Conjugation of PEG-AuNPs with oligonucleotides

The three oligonucleotide probes (ccpDNA, hcpDNA1 and hcpDNA2) were immobilized onto PEG-AuNPs by thiol-covalent binding. Briefly, for each DNA probe, 1 ml of PEG-AuNPs was added to 25 µl of DNA capture probe (10 µM in DEPC treated water). After 18 h of incubation time, the mixed solution was centrifuged twice at 6000 rpm for 20 min to remove the excess of oligonucleotide probe. The pellets were then re-dispersed in 200 µl Milli-Q water. The resultant colloidal solution was sonicated for 5 min and then stirred for 1 h at room temperature. When we grafted the different DNA probes (ccpDNA, hcpDNA1 and hcpDNA2), the NPs were still very stable without any precipitation even after several weeks. If we modified the surface chemistry of our AuNPs (AuNPs without PEG or without DNA probes), the AuNPs became unstable and we observed some precipitation of the AuNPs (Figure S2).

2.5 Detection of target oligonucleotides

Two reaction solutions were freshly prepared: one was the ccpDNA-AuNP solution and the other one was a mixed solution of equivalent volume of hcpDNA1-AuNP and hcpDNA2-AuNP solutions. Next, 5 µl of tDNA with different concentrations were added to 45 µl of reaction solution, which were then incubated at room temperature for 30 min. After the DNA hybridization, the reaction products were characterized by UV-Visible absorption spectroscopy. To determine the reproducibility of the detection, each experiment was reproduced 3 times and similar results were obtained.

2.6 UV/Visible measurements

The absorption spectra were recorded using a Thermo Scientific NanoDrop 2000/2000C UV-Visible spectrophotometer with an optical path of 10 mm. The wavelength range was 190–840 nm. All the measurements were carried out in a quartz cuvette using a sample volume of 50 µl.

2.7 Transmission electron microscopy (TEM)

The TEM images were recorded with a JEOL JEM 1011 microscope operating (JEOL, Tokyo, Japan) at an accelerating voltage of 100 kV. The operation details were realized as previously described [31].

3 Results and Discussion

Figure 1 illustrates the working principle for the detection of the tDNA using the two different strategies. First, AuNPs with a diameter of 10 nm were synthesized and then incubated with PEG. The obtained PEG-AuNPs exhibit an almost round shape and good monodispersity as characterized by the TEM images (Figure 2A). The PEG-AuNPs have a plasmon resonance at 521 nm (Figure 2B, black line) whereas the DNA-modified AuNPs displayed a redshift of a few nanometers, indicating the successful

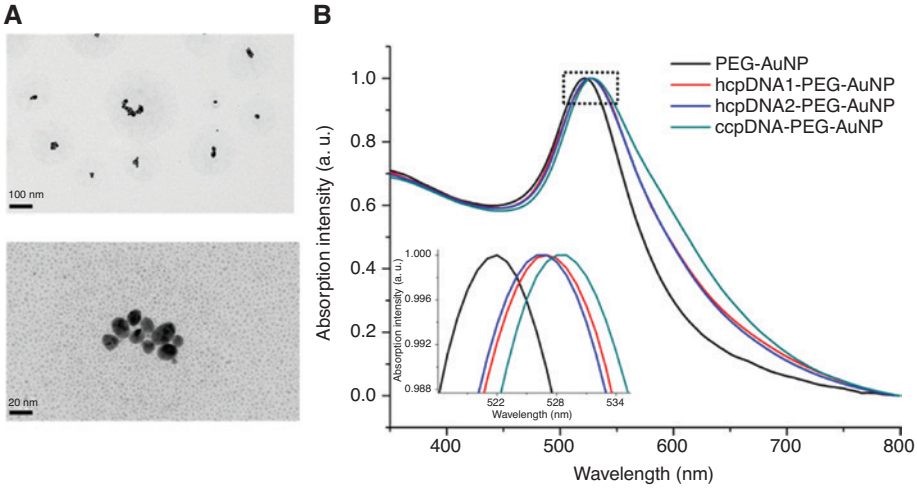

Figure 2: Characterization of AuNPs.
(A) The TEM images of the PEG-AuNP. (B) The UV-Visible absorbance spectra of the PEG-AuNPs (Black), the hcpDNA1-PEG-AuNPs (Red), the hcpDNA2-PEG-AuNPs (Blue), the ccpDNA-PEG-AuNPs (Green) and the mixture of the hcpDNA1-PEG-AuNPs and hcpDNA2-PEG-AuNPs (Orange).

functionalization of the PEG-AuNPs for each DNA capture probes. One can see that the grafting of hcpDNA1 and hcpDNA2 induces a similar redshift from 521 to 527 nm (Figure 2B, red and blue curves, respectively). The ccpDNA shows a larger shift from 521 to 529 nm (Figure 2B, green curve) as the ccpDNA has a longer length than the hcpDNA. For all the DNA capture probes, we also observe a shoulder on the higher wavelength side of the plasmon band that can be assigned to the formation of small aggregates in the solution. We assume that this is due to some electrostatic interactions between the DNA capture probes and the PEG of several AuNPs. In addition, the DNA-PEG-AuNPs maintained their red color as the PEG-AuNPs and had high stability and mono-dispersity. The short PEG molecules are found to promote the stability and performance of the ssDNA probes on gold surface without interfere with the DNA hybridization.

To detect the tDNA, we prepared two different solutions: one with the ccpDNA-PEG-AuNP (CCP method on Figure 1B) and one with a mixture of hcpDNA1-PEG-AuNP and of hcpDNA2-PEG-AuNP (MIX method on Figure 1C, the ratio between both hcpDNA-PEG-AuNP is 1:1). To these solutions we added different concentrations of tDNA (0 M,1 fM, 10 fM, 100 fM, 1 pM, 100 pM, 10 nM and 1 uM). For both the ccpDNA and hcpDNA mixture solutions, we observed that the shoulder intensity decreases when the concentration of the tDNA increases. This means that the interaction of the tDNA with the capture probes at the AuNPs' surface induces a disaggregation of the AuNPs related with the concentration of the tDNA (Figure 3A, B). As the position of the shoulder is similar for both methods (CCP and MIX ones), we assume that the AuNP aggregates should have the same size. Moreover, the addition of NaCl at different concentrations to the solution (Figure S3) induces a strong redshift of the LSPR band assigned to the aggregated NPs (the solution is no more stable with large precipitation after few hours). This proves that our NP can form large aggregates with the addition of NaCl before precipitation. This is also a clear evidence that our aggregation is limited in size as the aggregation band is only observed as a shoulder. In the case of the detection using the mixture of hcpDNA-PEG-AuNP, the detection is actually specific

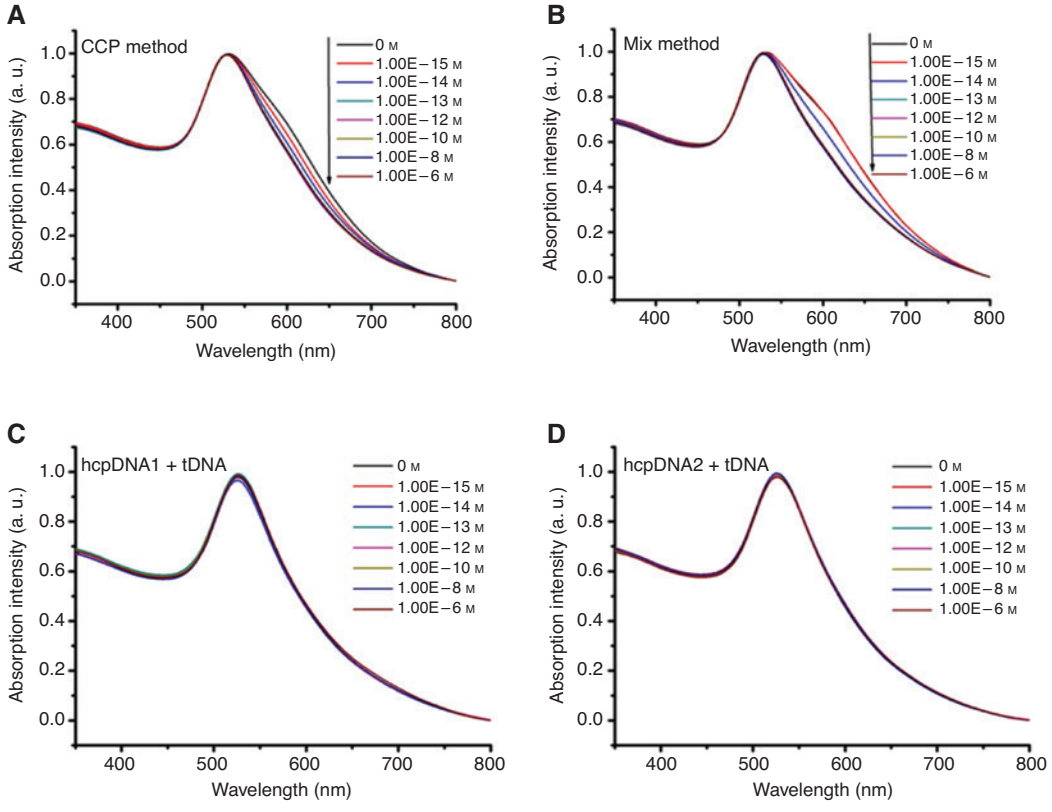

Figure 3: Two methods for tDNA detection.
The UV-Visible absorbance spectra of (A) ccpDNA-PEG-AuNPs and (B) the mixtures of hcpDNA-PEG-AuNPs for different concentrations of tDNA (0, 1 fM, 10 fM, 100 fM, 1 pM, 100 pM, 10 nM and 1 uM). The arrow indicates the decrease of the shoulder intensity with the increase of the tDNA concentrations. The UV-Visible absorbance spectra of hcpDNA1-PEG-AuNP (C) and hcpDNA2-PEG-AuNP (D) solutions for different concentrations of tDNA (0, 1 fM, 10 fM, 100 fM, 1 pM, 100 pM, 10 nM and 1 uM).

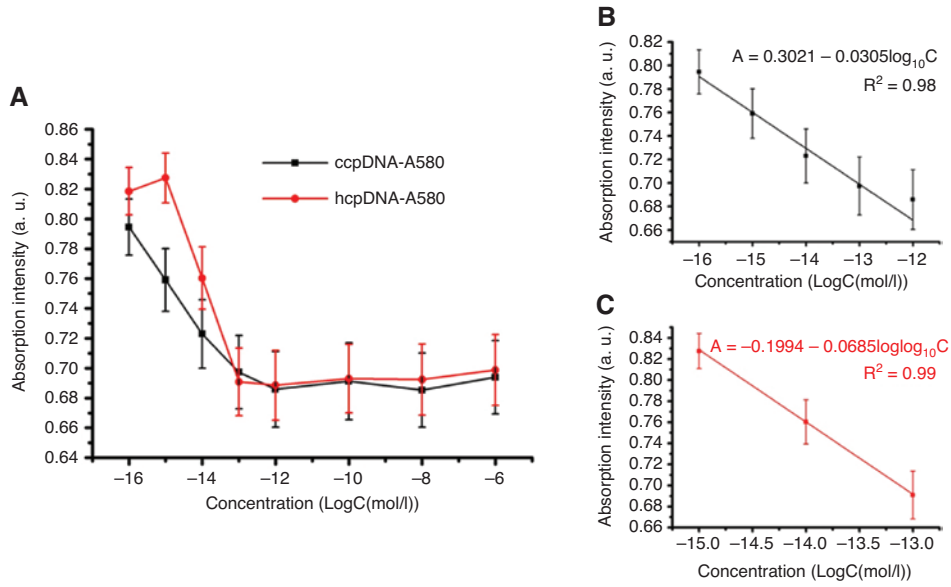

Figure 4: Quantitative test.
(A) The intensity of the shoulder at 580 nm (A580) versus the tDNA concentration for ccpDNA-PEG-AuNPs (black dots) and hcpDNA-PEG-AuNPs (red dots). (B) and (C) The linear fit of the A580 versus the logarithmic concentration of tDNA (B) from 10^{-15} to 10^{-12} M for ccpDNA-PEG-AuNPs and (C) 10^{-15}–10^{-13} M for the hcpDNA-PEG-AuNPs. The error bars are calculated using the values of the absorption intensity between 578 and 582 nm (580 ± 2 nm).

for the interaction of the tDNA with the mixed aggregates hcpDNA1-PEG-AuNP / hcpDNA2-PEG-AuNP. Indeed, when the tDNA is added to the solution with only one hcpDNA-PEG-AuNP (hcpDNA1 or hcpDNA2), no modification of the plasmon band is observed for any tDNA concentration (Figure 3C, D). Thus, when there is only hcpDNA1 or hcpDNA2, there is limited aggregation in the solution, and the tDNA does not interact with the nucleic acid probes at the AuNP surface.

In order to quantify the effect of the concentration of the tDNA on the shoulder intensity, we measured the intensity of the absorbance curve at 580 nm (A580) for the CCP and MIX methods (Figure 4) to provide the calibration curve of our detection methods. The A580 exhibits a linear variation of the logarithm (log) of the concentration of tDNA at low concentrations, across the range from a concentration lower than 10^{-15}–10^{-12} M with ccpDNA-PEG-AuNP and from 10^{-15} to 10^{-13} M with the hcpDNA-PEG-AuNP mixture (Figure 4A), spanning a response region of 4 and 2 orders of magnitude, respectively. For the higher concentrations, the intensity remains constant for both curves that exhibit a plateau. This means that no spectral modification is observable for concentrations higher than 10^{-12} M. The range of application of our sensor is then related to very low concentrations (fM and pM range).

In order to determine the sensitivity and the LoD, we fitted the linear part of each curve. The correlation equations are A580 = 0.3021–0.0305.log10(C) (R2 = 0.989) for the CCP method and A580 = 0.1945–0.0404.log10(C) (R2 = 0.955) for the MIX method, where C is the concentration of tDNA (Figure 4B, C). The sensitivity corresponds to the slopes of these fits: around −0.03 per decade for the CCP method and −0.04 per decade for the MIX method. The LoD was calculated using the standard methodology defined by the International Union of Pure and Applied Chemistry (IUPAC). The LoD is equal to ⟨xbl⟩ + k.σbl, where ⟨xbl⟩ is the mean of the blank measure, σbl is the standard deviation of the blank measure and k is a numerical factor (we take it equal to 3 to reach a confidence level of 95%). We obtain LoD values of 124 aM for the CCP method and of 2.54 fM for the MIX method.

To measure the concentrations, we also used another methodology based on the fit of the LSPR band (Section S1 and Figure S1a). We fitted the plasmon band with two peaks: one at 530 nm corresponding to the individual AuNPs and one at 580 nm assigned to the aggregates. We then plotted the intensity of the 580 nm peak versus the tDNA concentration (Figure S1b). The intensity change of the second band is similar to the trend observed with A580, which confirms our first conclusions. For this second method, the dots are more dispersed around the linear variation of the intensity. This higher dispersion of the dots can be due to the several data processing steps included in the fitting method, which introduces larger uncertainties on the calculated intensity of the second

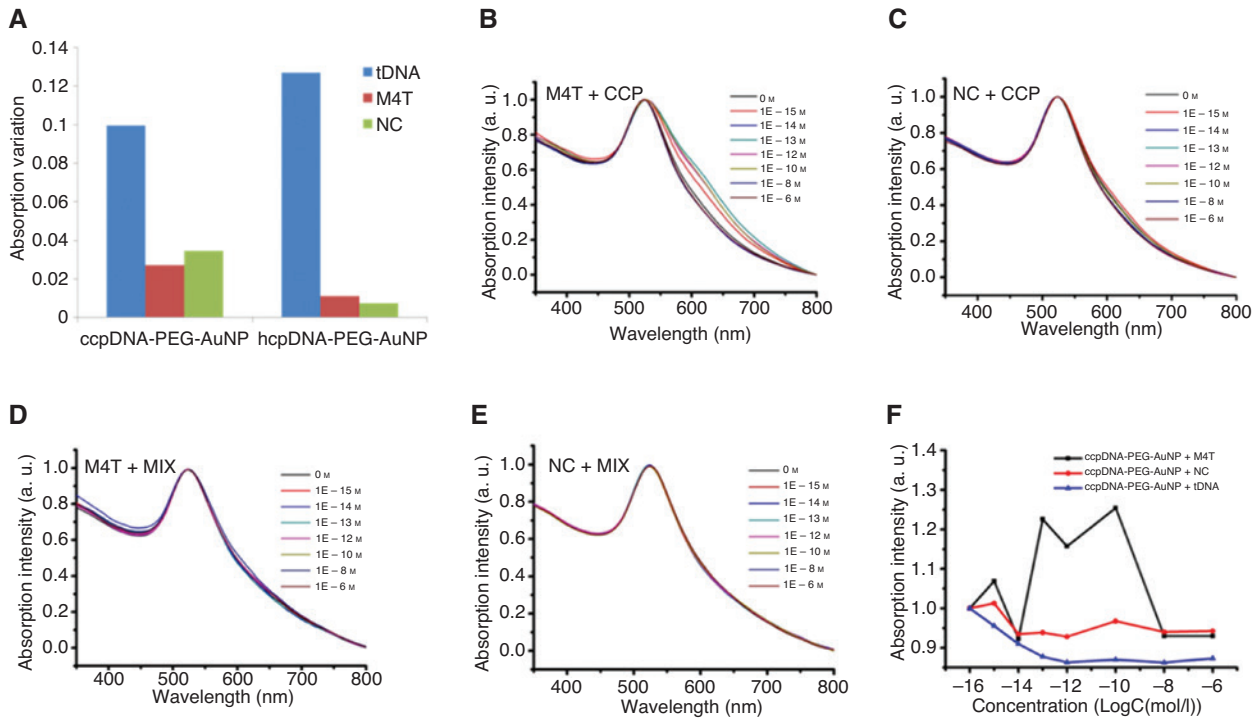

Figure 5: Specificity evaluation.
(A) The intensity at 580 nm for the tDNA and the two mismatched ssDNAs and for both detection methods. (B–E) The UV-visible spectra depending on the tDNA concentration for the following experiments: (B) M4T + CCP method, (C) NC + CCP method, (D) M4T + MIX method, (E) NC + MIX method. (F) The A580 intensity versus the ssDNA concentrations. The intensities were normalised by the A580 intensity measured with no tDNA.

peak. However, we believe that both methods are equivalent and provide similar results.

To evaluate the specificity of our detection methods, we performed control experiments with two other ssDNAs: one including four-base mismatched target oligonucleotide (M4T) and one involving non-complementary target oligonucleotide (NC). The sequences are listed in Table S1. As shown in Figure 5A, negligible A580 changes are observed for the two mismatched oligonucleotides with the MIX method, indicating the MIX method is highly selective. Only the tDNA induces spectral change and as a consequence can be detected by this method. For the NC with the CCP method, we observe the same behavior than with the MIX method, indicating that highly different ssDNAs cannot be detected by the CCP method. The addition of M4T causes some A580 variations for the CCP method, but no clear tendency can be observed in the A580 variation, and the modification of the A580 is essentially related to an increase of the A580 that could not be assigned to a non-specific detection (Figure 5F). Such "anomalous" trend can be explained by the unstable interaction between the M4T and the ccpDNA. Indeed, as the M4T has only four mismatches with the ccpDNA probe, they could interact together but this interaction is not strong enough to be stable. This should induce some unstable association and dissociation events and, as a consequence, a non-reproducible aggregation and disaggregation of the AuNP.

With all these data one can compare both methods. The CCP method has a larger range of application and a lower LoD (in the aM range), but it has a lower selectivity than the MIX method. Both methods are highly sensitive and allow reaching very low LoD in the fM range and even lower in others. This is largely lower than the common LoD observed for the LSPR methods [29] and is comparable to the PCR used to detect DNA. However, in this latter case, our method is largely faster (it only takes 30 min to complete detection), while the PCR needs at least 1 h. Our proposed method is also simpler to operate.

We assume that the performances of higher detection methods are related with the use of a PEG layer at the surface of the AuNPs. The PEG mainly plays two roles. It seems to make the hybridization with the target oligonucleotide more stable and it reduces the non-specific binding on gold surface, thus making the targeted DNAs more sensitive and specific to complementary target oligonucleotide.

4 Conclusion

In summary, we have developed an LSPR assay for rapid and simple methods that can be used for the detection of ssDNAs. Two detection methods were tested: one with a complete DNA CP and one with two half-sequence CPs. Both methods were validated for the detection of one ssDNA. We demonstrate that these methods are highly sensitive as we reached detection limits of 124 aM for the CCP method and 2.54 fM for the MIX method, which can satisfy the detection of low abundance DNA without combining other amplification strategies.

Compared with other detection methods, such as SERS, colorimetric, electrochemistry, fluorescence, etc., our method has unique advantages. A small volume of sample, rapid detection, simple operation and stable PEG-AuNP reagents make our method very suitable for point-of-care (POC) technology. In comparison, SERS and other methods which have high sensitivity require sophisticated instruments and professional analytical methods. Although the colorimetric method can be directly viewed, the sensitivity is far from being comparable to our method. Our method could be especially useful for diagnostic testing. In the future, it should be tested on clinical sample testing and its stability in clinical complexity needs to be further verified.

Acknowledgments: This work was supported by the National Key Basic Research and Development Plan 973 Project (2015CB 755400), by the National Natural Sciences Foundation of China (81430054, 81371641, 81601832), the Priority Projects of the Military Sciences Fund (BWS13C013) (SWH2017ZDCX4210), by the French National Research Agency (ANR) through the Louise project (ANR-15-CE04-0001) and the Nanobiosensor Project (ANR-15-CE29-0026).

References

[1] Lubin AA, Plaxco KW. Folding-based electrochemical biosensors: the case for responsive nucleic acid architectures. Acc Chem Res 2010;43:496–505.
[2] McGlennen RC. Miniaturization technologies for molecular diagnostics. Clin Chem 2001;47:393–402.
[3] Amos J, Patnaik M. Commercial molecular diagnostics in the U.S.: the Human Genome Project to the clinical laboratory. Hum Mutat 2002;19:324–33.
[4] van Belkum A. Molecular diagnostics in medical microbiology: yesterday, today and tomorrow. Curr Opin Pharmacol 2003;3:497–501.
[5] Saiki RK, Gelfand DH, Stoffel S, et al. Primer-directed enzymatic amplification of DNA with a thermostable DNA polymerase. Science 1988;239:487–91.
[6] Zhao Y, Chen F, Li Q, Wang L, Fan C. Isothermal amplification of nucleic acids. Chem Rev 2015;115:12491–545.
[7] Lizardi PM, Huang X, Zhu Z, Bray-Ward P, Thomas DC, Ward DC. Mutation detection and single-molecule counting using isothermal rolling-circle amplification. Nat Gene 1998;19:225–32.
[8] Hsieh K, Patterson AS, Ferguson BS, Plaxco KW, Soh HT. Rapid, sensitive, and quantitative detection of pathogenic DNA at the point of care through microfluidic electrochemical quantitative loop-mediated isothermal amplification. Angewandte Chemie 2012;51:4896–900.
[9] Huang J, Wu Y, Chen Y, et al. Pyrene-excimer probes based on the hybridization chain reaction for the detection of nucleic acids in complex biological fluids. Angewandte Chemie. 2011;50:401–4.
[10] Van Ness J, Van Ness LK, Galas DJ. Isothermal reactions for the amplification of oligonucleotides. Proc Nat Acad Sci USA 2003;100:4504–9.
[11] Lu N, Pei H, Ge Z, Simmons CR, Yan H, Fan C. Charge transport within a three-dimensional DNA nanostructure framework. J Am Chem Soc 2012;134:13148–51.
[12] Xia F, White RJ, Zuo X, et al. An Electrochemical supersandwich assay for sensitive and selective DNA detection in complex matrices. J Am Chem Soc 2010;132:14346–8.
[13] Wang F, Lu CH, Liu X, Freage L, Willner I. Amplified and multiplexed detection of DNA using the dendritic rolling circle amplified synthesis of DNAzyme reporter units. Analyt Chem 2014;86:1614–21.
[14] Zhang Y, Hu J, Zhang CY. Sensitive detection of transcription factors by isothermal exponential amplification-based colorimetric assay. Analyt Chem 2012;84:9544–9.
[15] Politi J, Spadavecchia J, Fiorentino G, Antonucci I, Casale S, Stefano LD. Interaction of Thermus thermophilus ArsC enzyme and gold nanoparticles naked-eye assays speciation between As(III) and As(V). Nanotechnology 2015;26:435703.
[16] Spadavecchia J, Moreau J, Hottin J, Canva M. New cysteamine based functionalization for biochip applications. Sens Actuators B Chem 2009;143:139–43.
[17] Guillot N, Lamy de la Chapelle M. Lithographied nanostructures as nanosensors. J Nanophotonics 2012;6:64506.
[18] Gillibert R, Huang JQ, Zhang Y, Fu WL, Lamy de la Chapelle M. Explosive detection by Surface Enhanced Raman Scattering. Trend Analyt Chem 2018;105:166–72.
[19] Gillibert R, Huang JQ, Zhang Y, Fu WL, Lamy de la Chapelle M. Food quality control by Surface Enhanced Raman Scattering. Trend Analyt Chem 2018;105:185–90.
[20] Gillibert R, Triba MN, Lamy de la Chapelle M. Surface enhanced Raman scattering sensor for highly sensitive and selective detection of ochratoxin A. Analyst 2017;143:339–45.
[21] Cottat M, D'Andrea C, Yasukuni R, et al. High sensitivity, high selectivity SERS detection of MnSOD using optical nanoantennas functionalized with aptamers. J Phys Chem C 2015;119:15532–40.
[22] David C, Guillot N, Hong S, Toury T, Lamy de la Chapelle M. SERS detection of biomolecules using lithographed nanoparticles towards a reproducible SERS biosensor. Nanotechnology 2011;21:475501.

[23] Tan E, Wong J, Nguyen D, et al. Isothermal DNA amplification coupled with DNA nanosphere-based colorimetric detection. Analyt Chem 2005;77:7984–92.
[24] He L, Musick MD, Nicewarner SR, et al. Colloidal Au-enhanced surface plasmon resonance for ultrasensitive detection of DNA hybridization. J Am Chem Soc 2000;122:9071–7.
[25] Su J, Wang D, Nörbel L, Shen J, et al. Multicolor gold–silver nano-mushrooms as ready-to-use SERS probes for ultra-sensitive and multiplex DNA/miRNA detection. Analyt Chem 2017;89:2531–8.
[26] Barbillon G, Bijeon JL, Plain J, Lamy de la Chapelle M, Adam PM, Royer P. Electron beam lithography designed chemical nanosensors based on localized surface plasmon resonance. Surface Sci 2007;601:5057–61.
[27] Barbillon G, Bijeon J-L, Plain J, Lamy de la Chapelle M, Adam P-M, Royer P. Biological and chemical gold nanosensors based on localized surface plasmon resonance. Gold Bull 2007;40:240–4.
[28] Thioune N, Lidgi-Guigui N, Cottat M, et al. Study of gold nanorods–protein interaction by localized surface plasmon resonance spectroscopy. Gold Bull 2013;46:275–81.
[29] Cottat M, Thioune N, Gabudean AM, et al. Localized surface plasmon resonance (LSPR) biosensor for the protein detection. Plasmonics 2013;8:699–704.
[30] Grand J, Adam PM, Grimault AS, et al. Optical extinction spectroscopy of oblate, prolate and ellipsoid shaped gold nanoparticles: experiments and theory. Plasmonics 2006;1:135–40.
[31] Guillot N, Lamy de la Chapelle M. The electromagnetic effect in surface enhanced Raman scattering: enhancement optimization using precisely controlled nanostructures. J Quant Spectrosc Radiat Transf 2012;113:2321–33.
[32] Zhou W, Gao X, Liu D, Chen X. Gold nanoparticles for in vitro diagnostics. Chem Rev 2015;115:10575–636.
[33] Sassolas A, Leca-Bouvier BD, Blum LJ. DNA biosensors and microarrays. Chem Rev 2008;108:109–39.
[34] Spadavecchia J, Movia D, Moore C, et al. Targeted polyethylene glycol gold nanoparticles for the treatment of pancreatic cancer: from synthesis to proof-of-concept in vitro studies. Int J Nanomed 2016;11:791–822.
[35] Degliangeli F, Kshirsagar P, Brunetti V, Pompa PP, Fiammengo R. Absolute and direct MicroRNA quantification using DNA–gold nanoparticle probes. J Am Chem Soc 2014;136:2264–7.

Supplementary Material: The online version of this article offers supplementary material (https://doi.org/10.1515/nanoph-2019-0050).